Plasma Chemistry and Plasma Processing, Vol. 14, No. 3, 1994

A Kinetic Study of Methane Conversion by a Dinitrogen Microwave Plasma

A. Oumghar,[1] J. C. Legrand,[1] A. M. Diamy,[1]
N. Turillon,[1] and R. I. Ben-Aïm[1]

Received June 12, 1993; revised September 29, 1993

Conversion of CH_4 with a N_2 microwave plasma (2.45 GHz) is studied. The experiments cover the absorbed microwave power range 300–700 W with 17–62% of methane in the gas mixture, with pressures of 10–40 mbar and flow rates of 140–650 $ml \cdot min^{-1}$. The yields of C_2 hydrocarbons and dihydrogen are analyzed by gas chromatography. The distance of methane addition downstream of the plasma plays an important role on the composition and the concentration of the products obtained. This distance mainly determines the energy concentrated in the active species of the plasma when they react with methane. Different behaviors for acetylene formation, on the one hand, and for ethane and ethene formation, on the other hand, have been observed, and this finding allows us to propose a kinetic mechanism for the decay of methane and for the formation of C_2 hydrocarbons.

KEY WORDS: Nitrogen microwave plasma; methane conversion.

1. INTRODUCTION

Reaction of methane with a nitrogen plasma is the subject of a great number of studies in various domains such as:

—simulation of Titan's atmosphere(1,2);
—detoxification of gases generated by combustion(3,4);
—properties and reactions of CN radical(5);
—metal coating(6);
—conversion of natural gas.(7)

The plasmas involved in these experiments are usually cold plasmas created either by microwave discharges,(4,5) RF discharges,(2,7) or by corona discharges.(1)

---

[1] Laboratoire de Chimie Générale, Université Pierre et Marie Curie, Case 196, 4, Place Jussieu, 75252 Paris Cedex 05, France.

0272-4324/94/0900-0239$07.00/0

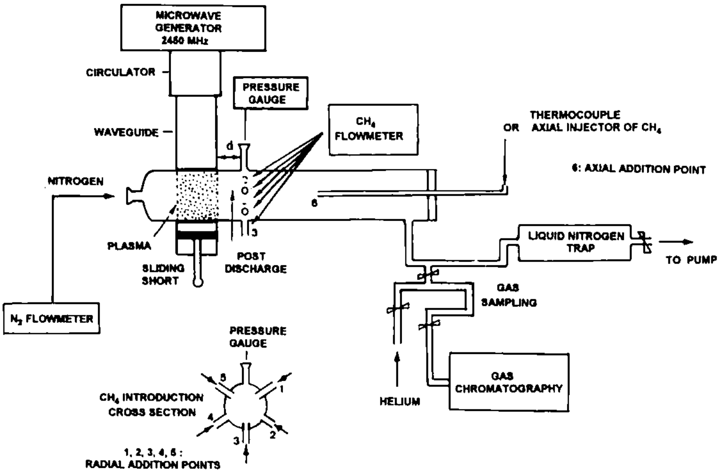

Fig. 1. Experimental setup.

The aim of our study is the direct conversion of methane in C_2 hydrocarbons. The present paper reports experimental results concerning methane transformation by means of a nitrogen microwave cold plasma and discusses the possible kinetic mechanism that governs the methane decomposition and the product formation on the basis of the comparison of kinetic constants given in the literature and on the basis of experimental results.

In a previous paper,(8) we have reported the experimental results obtained by introducing methane into the post-discharge zone of air microwave plasmas. A typical example is the following: the percentage of methane consumed is 82% and the yields (moles product/moles methane consumed) of acetylene, ethylene, ethane, hydrogen, and carbon monoxide are, respectively, 13, 2, 2, 90, and 62%; the carbon balance is 96%. The deficit can be attributed to formation of higher hydrocarbons and derivatives of hydrocyanic acid. An interesting feature is that, by choosing appropriate conditions, no solid carbon nor carbon dioxide is obtained even at a high conversion ratio. Now, we have simplified the reaction medium by using nitrogen instead of air in an attempt to determine the main reactions leading to product formation. Direct conversion of methane to C_2 hydrocarbons has generated widespread interest because of important industrial applications.(9)

2. EXPERIMENTAL

The experimental setup is shown in Fig. 1. A microwave generator (Thomson-CSF, 2.45 GHz, adjustable power up to 1500 W) is connected to a rectangular waveguide cavity of about 1 m length. Resonance is obtained by adjusting the position of a sliding short located at the end of the cavity. Stationary electromagnetic waves produce a plasma in a cylindrical reactor crossing the cavity. The reactor is made of fused silica and its inner diameter is 2.8 cm (o.d. = 3 cm). The part of the reactor located in the waveguide is small compared to the total volume of this last one. Thus, it is possible to assume the perturbation induced by the reactor to be weak, so when properly adjusted, the cavity could be operated in the empty cavity modes $TE_{0,1,n}$. At low pressure a surface wave propagates along the reactor; when the pressure rises ($P > 30$ torrs), a change of the propagation mode takes place and the plasma moves off the walls to occupy the central part of the reactor.

Incident (Π_i) and reflected (Π_r) powers are measured by a powermeter (HP 432A) connected to thermistors (HP 478A). Energy losses in the line are supposed to be negligible, so the energy absorbed by the gas is $\Pi = \Pi_i - \Pi_r$.

Methane is introduced into the plasma gas by means of five ports distributed all around the reactor (Fig. 1). Another port is used to measure the pressure P. The distance d separating the ports from the cavity can be modified between 0.9 and 4 cm by moving the reactor. Some experiments have been carried out with an axial injector (Fig. 1) so as to introduce methane into the cavity, except that in this case, a weak carbon deposition is observed on the reactor at the end of the discharge.

The pressure is measured by means of a baratron (MKS 122A). The static leakage rate for the whole setup is about 0.08 mbar/min. Research grade gases (99.995% minimum) are purchased from Air Liquide, and mass flowmeters (Alfagaz RDM 280) measure the gas flow rates F given in STP conditions, i.e., 298 K and 1 bar.

With this device, the following parameters have been investigated: consumption of methane α and of dinitrogen γ, and yields of products Y_x, defined as follows:

$\alpha = 100$ (moles of methane consumed/moles of methane introduced)
$\gamma = 100$ (moles of dinitrogen consumed/moles of dinitrogen introduced)
$Y_x = 100$ (moles of X produced/moles of methane consumed)

For carbon or hydrogen balance, selectivities of products S_x are obtained as $K \cdot Y_x$, where K is equal to 2 for C_2 hydrocarbons and 0.5 for dihydrogen.

The experimental variables are:

—flow of methane/flow of dinitrogen (β);
—the distance between the ports of methane introduction and the cavity (d);

—the pressure (P);
—the microwave power absorbed (Π);
—the gas flow (F).

Chemical analysis is performed by gas chromatography (Girdel 3000 with a thermal conductivity detector). Dinitrogen, methane, and dihydrogen are separated by a silicagel column (6.40 m long); ethane, ethylene, and acetylene are separated by a shorter column (1.80 m long). Traces of propane and butane are also detected. Nitriles and ammonia are trapped by silicagel columns, so they cannot be analyzed.

3. RESULTS

The experimental results are shown in Figs. 2–6. An important point is to determine if the chemical reactions occur as a consequence of the temperature increase or of the active species generated by the discharge. The effect of temperature on methane pyrolysis has been extensively studied. Without a catalyst, no direct conversion is produced under 1000°C; for a stoichiometric CH_4/O_2 mixture, oxidation is detected at 550°C.(9) We have measured the temperature of the plasma at the point of mixing with methane, by means of a Pt–10%Rh/Pt thermocouple coated with silica (Fig. 2). It is in the range 300–800°C in the usual conditions; it is about 900°C only when the maximum value of the microwave power is used. So it can be assumed that the reactions occurring in this CH_4/N_2 system are initiated by the active species of the discharge.

From Figs. 3–6, it turns out that the main features are the following:

—acetylene and dihydrogen are not obtained if d is longer than 2 cm. In the same way, acetylene was missing for $d > 2$ cm in the work previously mentioned and carried out with an air plasma(8);
—yields of ethane and ethylene are very similar functions of the different parameters;
—if the distance d is longer than 3.2 cm, C_2 hydrocarbons are not obtained though methane is still consumed. It must be supposed that HCN, nitriles, and NH_3 are formed as observed by Raulin *et al.*(1) and Thomson *et al.*(2)
—as expected, dinitrogen decay hardly varies as a function of β since the experimental conditions of the microwave discharge remain the same while the flow of methane varies.

The distance d is a factor determining the time necessary for the active species of the plasma to meet methane. This time of flight can be estimated between 0 (when methane is introduced in the end of the luminous part of

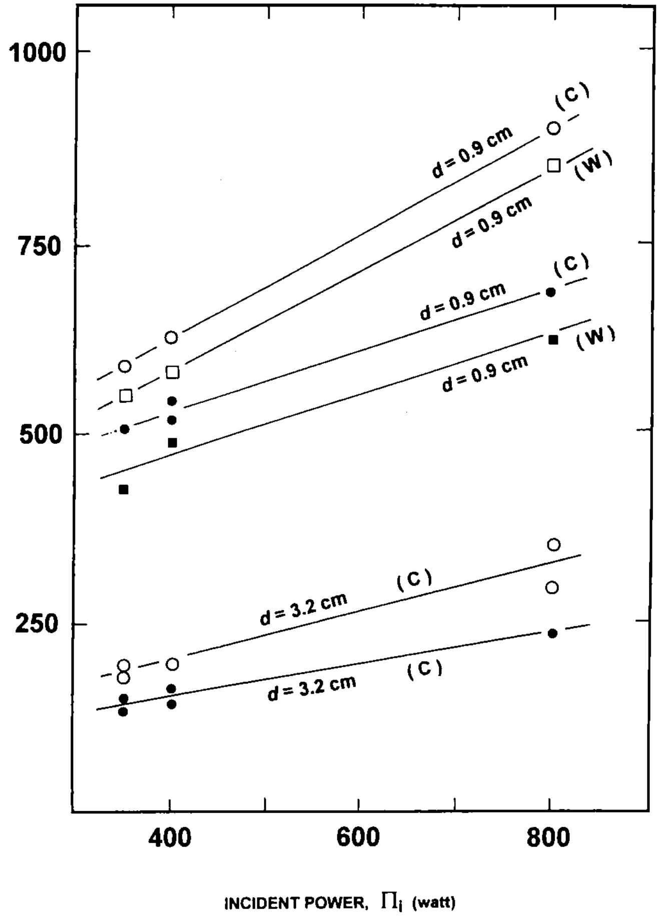

Fig. 2. Kinetic temperature of the gas versus incident power Π_i. $F=350$ ml STP/min; $P=13.2$ mbar; $\beta=2/5$. ○, □: pure dinitrogen plasma; ●, ■: dinitrogen plasma + methane. C: center; W: near the wall.

the plasma) and 3 ms (when $d=3.2$ cm, $P=10$ mbar, and $F=140$ ml STP·min^{-1}). According to the lifetime of each active species, the composition of the system is modified with d; so the distance d is also a factor determining the nature of the products.

As suggested by the experimental results, three different zones for introduction of methane must be considered:

—end of the plasma: all the chemically active species plus energetic electrons are present; the electron temperature measured by means of a floating double probe$^{(10)}$ is of the order of 10^4 K (zone A);

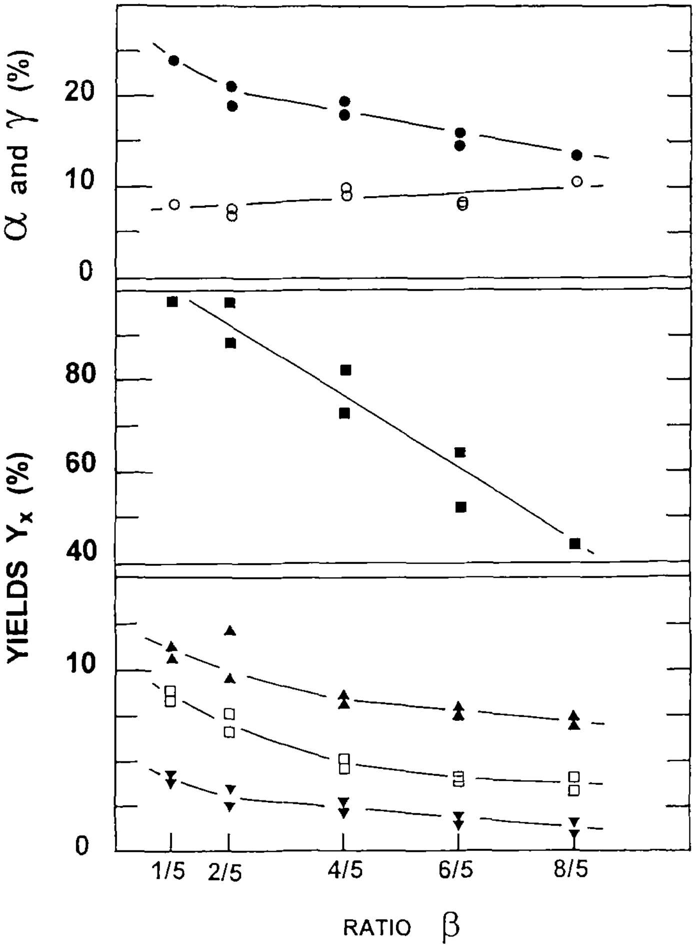

Fig. 3. Methane conversion α(%), dinitrogen decay γ(%), and yields Y_x(%) versus methane/dinitrogen ratio β. Radial introduction; $F = 300$–650 ml STP/min; $d = 0.9$ cm; $P = 13.2$ mbar; $\Pi_i = 370$ W. ●: CH_4; ○: N_2; ■: H_2; ▲: C_2H_2; □: C_2H_6; ▼: C_2H_4.

—intermediate distances: (2–3 cm) corresponding to the beginning of the post-discharge; energetic electrons have disappeared (zone B);

—attenuated post-discharge ($d > 3$ cm): the active species remaining are those having long lifetimes (zone C).

As part of an applied study concerning conversion of methane,(8) we have tried to obtain better acetylene yields by introducing methane into the plasma and by increasing pressure. To reduce the distance *d*, it was necessary

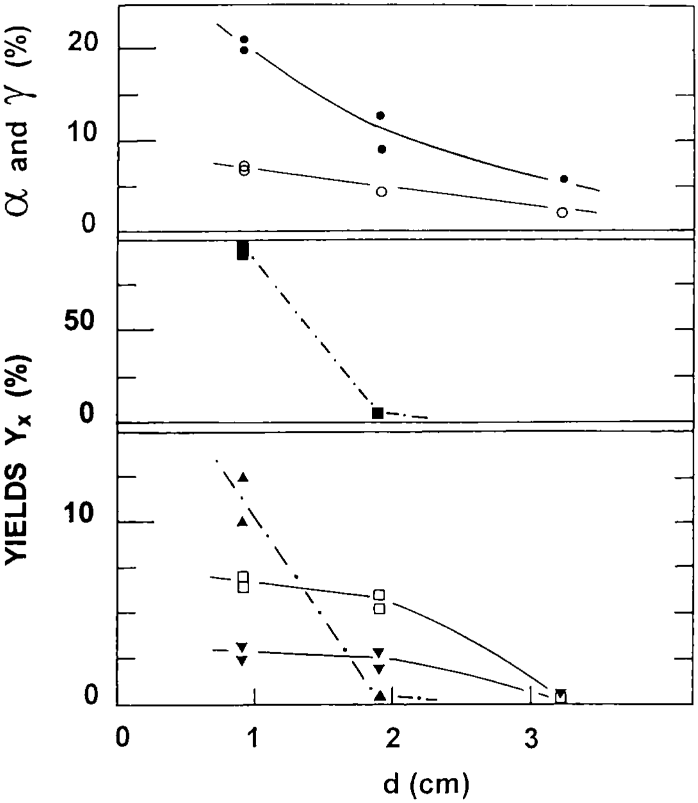

Fig. 4. Methane conversion α(%), dinitrogen decay γ(%), and yields Y_x(%) versus distance d of methane addition after the cavity. Radial introduction; $F = 350$ ml STP/min; $\beta = 2/5$; $P = 13.2$ mbar; $\Pi_i = 370$ W. ● : CH_4 ; ○ : N_2 ; ■ : H_2 ; ▲ : C_2H_2 ; □ : C_2H_6 ; ▼ : C_2H_4.

to use an axial introduction composed of a cylindrical tube with a pepperpot ending, as shown in Fig. 1. In Figs. 6 and 7, C_2 hydrocarbon ratios (moles of hydrocarbon formed/moles of methane introduced) are shown as a function of pressure and distance of methane introduction. Again, it appears that acetylene behaves differently from the other two C_2 hydrocarbon behaviors. Raising pressure or decreasing introduction distance leads to an increase of acetylene production but has little influence on ethylene and ethane production.

Below, we investigate the following on the basis of thermodynamic and kinetic data:

—the active species of the plasma (discharge and post-discharge) and the reactions between these species and methane;

—the reactions of formation of C_2 hydrocarbons and other products.

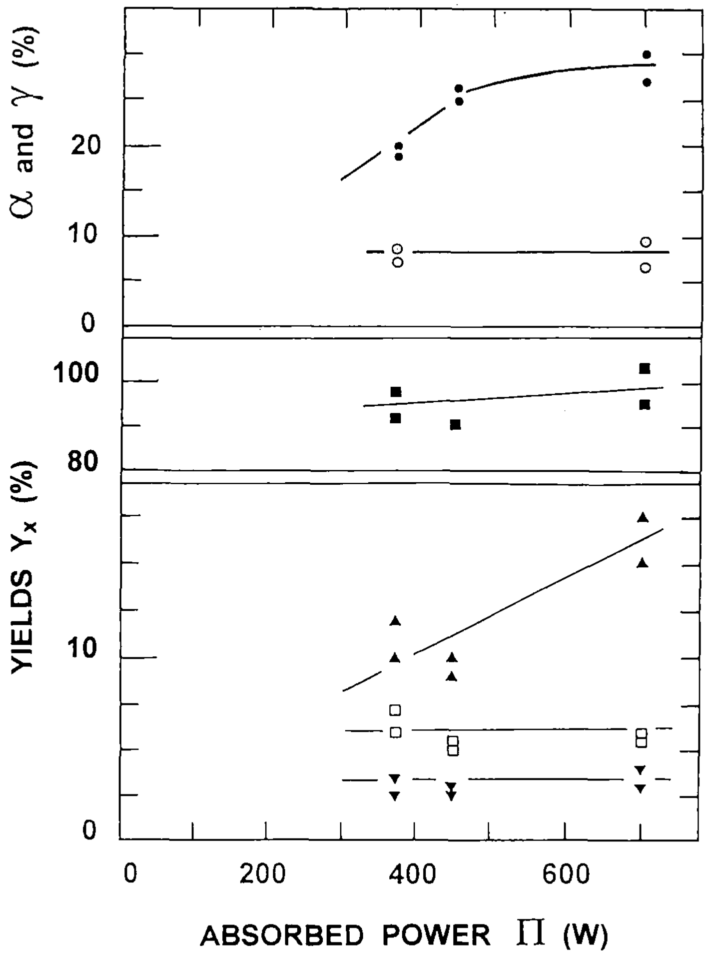

Fig. 5. Methane conversion α(%), dinitrogen decay γ(%), and yields Y_x(%) versus absorbed microwave power Π. Radial introduction; $F = 350$ ml STP/min; $\beta = 2/5$; $P = 13.2$ mbar; $d =$ 0.9 cm. ● : CH_4 ; ○: N_2 ; ■: H_2 ; ▲ : C_2H_2 ; □: C_2H_6 ; ▼ : C_2H_4.

4. REACTION MECHANISM

In this section, we discuss the reactions considered relevant to explain the decomposition of methane and C_2 hydrocarbon formation in the system studied here. Table I shows rate constants involved in the following kinetic scheme, and Table II shows standard enthalpies of formation of species that might form during methane conversion processes. Thermodynamic data do not govern the chemical mechanism and the rate law of methane conversion

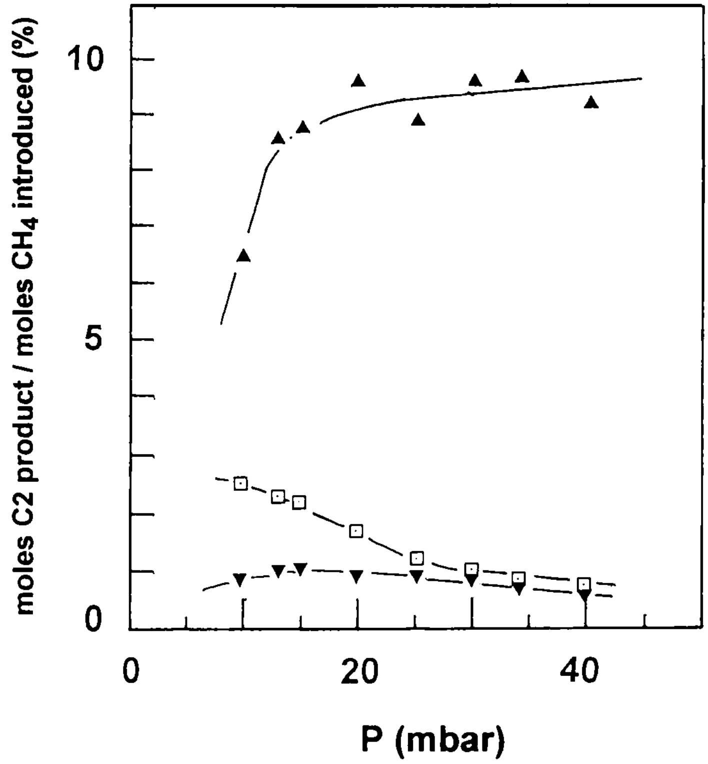

Fig. 6. Moles C_2 product/moles CH_4 introduced versus pressure *P*. Radial introduction; *F*= 140 ml STP/min; $\beta = 2/5$; $d = 0.9$ cm; $\Pi = 290$ W. ▲ : C_2H_2 ; □: C_2H_6 ; ▼ : C_2H_4.

but may provide some information. Due to the experimental results, some global endothermal reactions can be taken into account, such as

$$\begin{aligned}
&2CH_4 = C_2H_2 + 3H_2, && \Delta H^\circ = 376.5\ \text{kJ}\\
&2CH_4 = C_2H_4 + 2H_2, && \Delta H^\circ = 202.3\ \text{kJ}\\
&2CH_4 = C_2H_6 + H_2, && \Delta H^\circ = 65.1\ \text{kJ}\\
&CH_4 + 0.5N_2 = HCN + 1.5H_2, && \Delta H^\circ = 210.0\ \text{kJ}\\
&CH_4 + N_2 = HCN + NH_3, && \Delta H^\circ = 164.1\ \text{kJ}
\end{aligned}$$

Obviously, initiation of methane decomposition requires species with an energy high enough to break a H–CH_3 bond and a lifetime long enough to be present when methane is introduced. Generally, these two conditions are opposite and are fulfilled only by a few species. In the following section we survey the main species of the nitrogen plasma fulfilling these conditions.

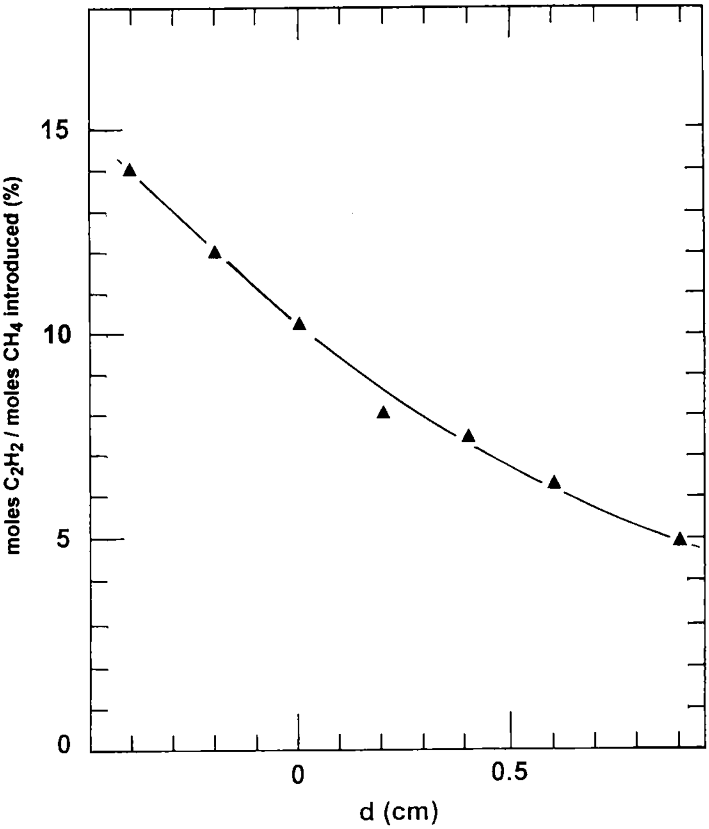

Fig. 7. Moles C_2H_2/moles CH_4 introduced versus distance *d* of methane addition after the cavity using the axial introduction of methane. $F = 170$ ml STP/min; $\beta = 7/10$; $P = 25$ mbar; $\Pi = 290$ W.

4.1. Initiation Reactions

It is well known that molecular nitrogen subjected to the action of an electrical discharge is very reactive chemically. This reactivity is mainly due to vibrationally excited molecules in the ground electronic state ($X'^1\Sigma_g^+$, v), electronically excited molecules in metastable states ($A^3\Sigma_u^+$), ($a'^1\Sigma_u^-$), ($a^1\Pi_g$), and N atoms in the ground state (^4S) or in the metastable states (^2D) or (^2P). Ions (mainly N^+, N_2^+, N_3^+) and also electrons can account for the reactivity of the medium.(11)

Radiative species such as $N_2(C^3\Pi_u)$, $N_2(B^3\Pi_g)$, $N_2^+(B^2\Sigma_u^+)$ are responsible for the greater part of the spectra of nitrogen; but due to their short radiative lifetime their contribution to the chemical reactivity of discharged nitrogen is not large.

Table I. Kinetic Data

Number	Reactants		Products	k (ml · molecule^{-1} · s^{-1})	Temperature range (K)	Reference
1	$CH_4 + e(\varepsilon > 10\ eV)$	→	$CH_4\ (S_1, S_2)$	$k = f(T_e)$		13
2a	$CH_4 + N_2(A, v = 1)$	→	products	1.5×10^{-12}		14
2b	—	→	$CH_3 + HN_2$			17
3	$CH_4 + N_2(X, v > 20)$	→	$CH_3 + H + N_2$			
4	$CH_4 + N$	→	$CH_3 + NH$	$1.7 \times 10^{-11} \exp(-12000/T)$ (estimated)		24
5	$CH_4 + N_2^+$	→	products	1.3×10^{-9}		30
6	$CH_4 + N^+$	→	products	1.1×10^{-9}		30
7	$CH_3 + CH_3$	$\xrightarrow{M}$	C_2H_6	$k_\infty = 4.0 \times 10^{-10} \times T^{-0.4}$	300–2000	32
8	$CH_3 + CH_3$	→	$C_2H_4 + H_2$	$1.7 \times 10^{-8} \exp(-16000/T)$	1500–2500	32
9	$CH_2 + CH_2$	→	$C_2H_4^*$	1.7×10^{-12}		33
10	$CH_3 + {}^1CH_2$	→	$C_2H_4 + H$	3.0×10^{-11}		37
11	$CH_3 + {}^3CH_2$	→	$C_2H_4 + H$	7.0×10^{-11}	300–3000	23
12	$CH_4 + CH$	→	products	$5.0 \times 10^{-11} \exp(200/T)$	200–700	23
13	$C_2H_5 + CH_3$	→	$C_2H_4 + CH_4$	1.9×10^{-12}	300–800	23
14	$C_2H_5 + C_2H_5$	→	$C_2H_6 + C_2H_4$	2.4×10^{-12}	300–1200	23
15	$C_2H_6 + N_2(A, v = 1)$	→	products	3.6×10^{-12}		14
16	$C_2H_6 + N_2(X, v)$	→	products			
17	$C_2H_6 + H$	→	$C_2H_5 + H_2$	$2.4 \times 10^{-15} \times T^{1.5} \exp(-3730/T)$	300–2000	23
18	$CH_3 + CH_3$	→	$C_2H_5 + H$	$1.3 \times 10^{-9} \exp(-13275/T)$	1500–3000	32
19	$C_2H_6 + CH_3$	→	$CH_4 + C_2H_5$	$2.5 \times 10^{-31} \times T^{6.0} \exp(-3043/T)$	300–1500	23
20	$CH_2 + CH_2$	→	$C_2H_2 + H_2$ (or 2H)	$2.0 \times 10^{-10} \exp(-400/T)$	300–3000	23
21	$CH + CH$	→	C_2H_2	2.0×10^{-10}		38
22	$CH_3 + C$	→	$C_2H_2 + H$	8.3×10^{-11}		24
23	$CH_2 + CH$	→	$C_2H_2 + H$	6.6×10^{-11}		24
24	$CH_3 + N$	→	$HCN + H_2$	1.4×10^{-11}	363	25
25	$CH_2 + N$	→	$HCN + H$	8.3×10^{-11} (estimated)		24
26	$CH_2 + NH$	→	$HCN + 2H$	5.0×10^{-11} (estimated)		24
27	$CH + NH$	→	$HCN + H$	8.3×10^{-11} (estimated)		24
28	$CH_4 + CN$	→	$HCN + CH_3$	$7.0 \times 10^{-13}(T/298)^{2.3} \exp(16/T)$	295–700	39
29	$H_2 + CN$	→	$HCN + H$	$5.0 \times 10^{-19} \times T^{2.45} \exp(-1118/T)$		40
30	$N_2^+ + H_2$	→	$N_2H^+ + H$	1.8×10^{-9}		30
31	$N_2^+ + H$	→	N_2H^+			36
32	$N_2H^+ + e$	→	$NH + H$			36
33	$N_{(ads)} + H$	→	$NH_{(ads)}$			35
34	$H + CH_4$	→	$H_2 + CH_3$	$2.2 \times 10^{-20} \times T^{3.0} \exp(-4045/T)$	300–2500	23
35	$C_2H_5 + CH_3$	$\xrightarrow{M}$	C_3H_8	$k_\infty = 4.7 \times 10^{-11}$	300–800	23
36	$C_2H_5 + C_2H_5$	$\xrightarrow{M}$	C_4H_{10}	$k_\infty = 1.9 \times 10^{-11}$	300–1200	23
37	$CH_3 + N$	→	$H_2CN + H$	1.3×10^{-10}	363	25
38	$H_2CN + N$	→	$HCN + NH$	6.7×10^{-11}	363	25
39	$CH + NH_2$	→	$HCN + 2H$	5.0×10^{-11} (estimated)		24
40	$CH_2 + N_2$	→	products	$< 10^{-16}$		37
41	$CH + N_2$	→	products	$1.7 \times 10^{-14} \exp(975/T)$	297–675	41
42	$CH_4 + N(^2D)$	→	products	1.5×10^{-12}	300	27
43	$C + N_2$	→	$CN + N$	$1.1 \times 10^{-10} \exp(-23000/T)$		40
44	$CH + N$	→	$CN + H$	2.1×10^{-11}		26
45	$CH_2 + N$	→	$CH + H_2$	1.6×10^{-11}		42

Table II. Thermodynamical Data

Molecules	Atoms, ions, radicals	Enthalpy of formation (1 bar, 298 K), kJ/mole	Reference
	N_2^+	1509.5	44
$CH_4(S_2)$		1128.8	12
$CH_4(S_1)$		926.2	12
$N_2(X, v)$		0-945.4	
	C_2(gas)	837.7	44
	C(gas)	717.7	44
$N_2(A, v=0)$		598.2	14
	CH	594.1	44
	N	472.7	44
	CN	435.1	44
	CH_2	386.4	44
	NH	376.6	44
C_2H_2		226.7	44
	H	218.0	44
	NH_2	190.4	44
	CH_3	145.7	44
HCN		135.1	44
N_2H_4		95.4	44
C_2H_4		52.5	44
C(solid), H_2		0	
NH_3		−45.9	44
CH_4		−74.9	44
C_2H_6		−84.7	44

Now we will examine the species with sufficient energy, concentration, and lifetime to induce the decomposition of methane.

4.1.1. Electrons

The study of electron-methane collisions by Nectoux *et al.*(12) points out that electronically excited methane S_1 (9.6 and 10.4 eV) and S_2 (11.7 eV) are the precursors of the products due to an electron collision to give CH_3, CH_2, CH, and C according to the following reactions:

$$e(\varepsilon > 10\,\text{eV}) + CH_4 \rightarrow CH_4(S_1, S_2) + e \qquad (1)$$

$$CH_4(S_1, S_2) \rightarrow \begin{cases} CH_3 + H & (1a) \\ CH_2 + H + H & (1b) \\ CH_2 + H_2 & (1c) \\ CH + H_2 + H & (1d) \\ C + H_2 + H_2 & (1e) \end{cases}$$

For collision of methane with species, such as electrons, it is possible to assume an activation energy of about 9.6 eV; when a species is able to react with methane via a transition state, the activation energy may be appreciably lower.

Cross-sections for dissociation of methane by electron collisions have been reviewed by Morgan.(13) With these data we have computed the corresponding rate constant as a function of electron temperature (Fig. 8). It turns out that when methane is introduced near or into the discharge, electrons can participate in initiation of the reaction. As, upon increase of the injection distance, electron temperature and density rapidly decrease, collisions with electrons will be of lesser importance in the chemical reactivity of the system.

4.1.2. *Metastable $N_2(A)$*

The metastable $N_2(A)$ is produced in the discharge by collisions with electrons and also radiatively from the $B^3\Pi_g$ state. In its zero vibrational level, this metastable molecule is 6.2 eV above the ground state, and its radiative lifetime is about 2 s.(14) Thus, this species is able to break the bonds of many organic molecules. Golde *et al.*(15) have investigated the quenching of vibrational states ($v=0$ to $v=6$) of $N_2(A)$ by methane; they have observed the presence of hydrogen as a consequence of quenching. Thus, the metastable molecule $N_2(A)$ is a possible candidate for initiation of decomposition of methane:

$$CH_4+N_2(A, v) \rightarrow CH_3+H+N_2 \tag{2a}$$

$$CH_4+N_2(A, v) \rightarrow CH_3+HN_2 \tag{2b}$$

Reaction (2a) has also been pointed out by Wright *et al.*(16) in studies dealing with active nitrogen. Reaction (2b) needs about the same energy as (2a), but reaction (2b) gives the radical HN_2 which has a very short lifetime, greatly limiting its role in the mechanism.(17)

4.1.3. *Dinitrogen $N_2(X, v)$*

In dinitrogen, large transfer rates of e–v processes during electron–molecule collisions populate the vibrational levels, and large vibrational transfer rates (v–v processes) are associated with unusually low vibrational–translational transfer rates (v–t processes).(18,19) Moreover, vibrational states for a homonuclear molecule are metastable. Thus, in dinitrogen, the population of the 46 vibrational levels is important, and they have a long lifetime. As these vibrational levels are not easily quenched on the wall, it is possible to find these active species far in the post-discharge.(20) The dissociation energy of a –C–H bond in methane is 4.5 eV and this energy tallies with

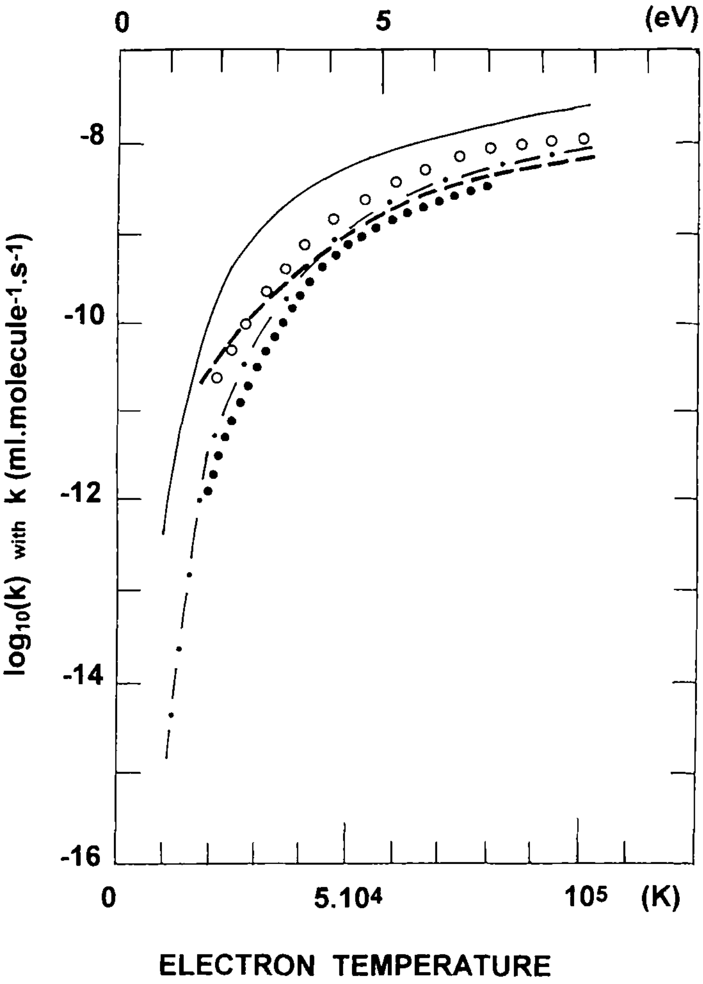

Fig. 8. Kinetic constants k of ionization or dissociation by electron impact versus electron temperature (K or eV). Constants k are calculated from Refs. 13 and 43. ○: $N_2+e=2N+e$; ●: $N_2+e=N_2^++2e$; - - -: $N+e=N^++2e$; — · —: $CH_4+e=CH_4^++2e$; ——: $CH_4+e=$ products.

vibrational levels for $v=20$. As an example, Capitelli *et al.*(19) have calculated a concentration of about 2×10^{14} molecule/ml for v between 20 and 40 for a pressure of about 4 mbar, a gas temperature of 1000 K, an electron temperature of 20,000 K, and after a time of 1 ms. Thus, the following reaction can be retained as initiation reaction:

$$CH_4+N_2(X, v>20) \rightarrow CH_3+H+N_2 \qquad (3)$$

4.1.4. Metastable $N_2(a')$ and $N_2(a)$

The energies of these states are, respectively, 8.52 and 8.67 eV, with lifetimes of about 13 to 500 μs for $(a')$$^{(21)}$ and 80 μs for (a).$^{(22)}$ Thus, these states have an energy high enough to break a $H_3C–H$ bond. Rate constants for quenching of $N_2(a')$ and $N_2(a)$ by methane have been measured.$^{(22)}$ Dissociation of methane is a probable way of quenching, as for quenching of $N_2(A)$. Concentrations of these species in a microwave plasma are not known, but we can assume that $[N_2(a')]$ or $[N_2(a)] \ll [N_2(A)]$, so it appears that their chemical reactivity is negligible regarding $N_2(A)$ chemical reactivity.

4.1.5. Nitrogen Atoms $N(^4S)$, $N(^2D)$, and $N(^2P)$

Dinitrogen dissociation in a microwave discharge reaches a few percent.$^{(20)}$ Ground-state atoms have a low recombination rate constant in the gas phase in our experimental conditions (relatively high temperature and low pressure)$^{(23)}$ and a low recombination coefficient on silica.$^{(20)}$ Thus, under these conditions, they may survive for a long time after the discharge; their presence in the afterglow and their chemical reactivity have been demonstrated for some time.$^{(11)}$ However, the rate constant of the following reaction is low$^{(24)}$:

$$CH_4 + N(^4S) \rightarrow CH_3 + NH \tag{4}$$

so $N(^4S)$ does not participate to a great extent in the initiation of the reaction but exhibits high rate constants with CH_x radicals,$^{(24,25,26)}$ and consequently $N(^4S)$ may play an important role in product formation.

In contrast, $N(^2D)$ shows a higher rate constant of reaction with methane (Table I)$^{(27,28)}$ but a concentration several orders of magnitude lower than $N(^4S)$; as an example, in a positive column the ratio $[(^2D)+(^2P)]/[(^4S)]$ is about 10^{-3}.$^{(20)}$ $N(^2P)$ atoms are less reactive than $N(^2D)$,$^{(29)}$ so the chemical contribution of nitrogen atoms would be negligible for initiation reactions.

4.1.6. Ions

Ion reactivity is important with methane since the following reactions have high rate constants$^{(30)}$:

$$CH_4 + N_2^+ \rightarrow N_2 + CH_3^+ + H \tag{5}$$

$$CH_4 + N^+ \rightarrow CH_3^+ + NH \tag{6}$$

These reactions can take place when methane is introduced into or very near the discharge, but it is necessary to remember that ion concentrations are about 10^{11} or 10^{12} molecule/ml; so their role cannot be important in this system. Moreover, Hiraoka *et al.*(31) have shown that in an rf discharge the formation of the main products arising from methane decomposition proceeds by a radical mechanism rather than an ionic one. We may thus conclude that the main species for initiation reactions are electrons, $N_2(A)$ and $N_2(X, v)$.

4.2. Product Formation

In this section, we investigate the main reactions that can lead to products under our experimental conditions.

4.2.1. Ethane

According to the literature,(32) the main reaction leading to ethane, with participation of primary radicals coming from methane, is the recombination of two methyl radicals:

$$CH_3 + CH_3 \xrightarrow{M} C_2H_6 \tag{7}$$

This reaction shows a rate constant of a reasonable order of magnitude under our experimental conditions (Table I).

Ethane can be dissociated, in the same way as methane, to produce ethyl radicals, which in turn give ethane through reaction (14), as explained further.

4.2.2. Ethylene.

Several reactions can lead to ethylene:

$$CH_3 + CH_3 \rightarrow C_2H_4 + H_2 \tag{8}$$

$$CH_2 + CH_2 \rightarrow C_2H_4^* \tag{9}$$

$$CH_3 + {}^1CH_2 \rightarrow C_2H_4 + H \tag{10}$$

$$CH_3 + {}^3CH_2 \rightarrow C_2H_4 + H \tag{11}$$

$$CH_4 + CH \rightarrow C_2H_4 + H \tag{12}$$

$$C_2H_5 + CH_3 \rightarrow C_2H_4 + CH_4 \tag{13}$$

$$C_2H_5 + C_2H_5 \rightarrow C_2H_6 + C_2H_4 \tag{14}$$

The rate constant of reaction (8) is very small under our experimental conditions compared to reaction (7). Recombination of two methylene radicals CH_2 leads preferably to acetylene formation [reaction (20)]. Indeed, Mackie and Doolan(33) have estimated $k_9 (k_9 \ll k_{20})$ and Braun *et al.*(34) have concluded that reaction (9) is negligible in a study of CH_2 reactions. Thus, the main reactions in ethylene formation are reactions (10)–(14).

Ethyl radicals can result from ethane decomposition by electron impact or by active nitrogen(11,14,18) through reactions such as

$$C_2H_6 + N_2(A) \rightarrow C_2H_5 + H + N_2 \tag{15}$$

$$C_2H_6 + N_2(X, v) \rightarrow C_2H_5 + H + N_2 \tag{16}$$

It is possible that $N_2(X, v)$ may play the same role as $N_2(A)$ in the dissociation of ethane when v is high enough.

On the contrary, the following reactions seem unlikely because their rate constants are too low:

$$C_2H_6 + H \rightarrow C_2H_5 + H_2 \tag{17}$$

$$CH_3 + CH_3 \rightarrow C_2H_5 + H \tag{18}$$

$$C_2H_6 + CH_3 \rightarrow C_2H_5 + CH_4 \tag{19}$$

4.2.3. *Acetylene*

The main reaction leading to acetylene is

$$CH_2 + CH_2 \rightarrow C_2H_2 + H_2 \text{ (or 2H)} \tag{20}$$

Braun *et al.*(34) have also considered CH radical recombination:

$$CH + CH \rightarrow C_2H_2 \tag{21}$$

The reactions below can also be taken into account; high rate constants have been estimated:

$$CH_3 + C \rightarrow C_2H_2 + H \tag{22}$$

$$CH_2 + CH \rightarrow C_2H_2 + H \tag{23}$$

4.2.4. *HCN and NH_3*

Many reactions involving CH_4 or CH_x radicals can account for HCN formation in the three reaction zones (see Table I); the main ones are

$$CH_3 + N \rightarrow HCN + H_2 \text{ (or 2H)} \tag{24}$$

$$CH_2 + N \rightarrow HCN + H \tag{25}$$

$$CH_2 + NH \rightarrow HCN + 2H \tag{26}$$

$$CH + NH \rightarrow HCN + H \tag{27}$$

$$CH_4 + CN \rightarrow HCN + CH_3 \tag{28}$$

$$H_2 + CN \rightarrow HCN + H \tag{29}$$

NH_3 formation has been studied in discharges by Venugopalan *et al.*(35) and also by Uyama *et al.*(36); NH radicals are considered ammonia precursors. These radicals are mainly formed in the discharge through the following reactions:

$$N_2^+ + H_2 \rightarrow N_2H^+ + H \tag{30}$$

$$N_2^+ + H \rightarrow N_2H^+ \tag{31}$$

$$N_2H^+ + e \rightarrow NH + H \tag{32}$$

In the post-discharge, under our experimental conditions, N or H atoms do not recombine in the gas phase but on the wall. N atoms absorbed on the wall combine with hydrogen from the gas phase or from the surface to form successively NH and NH_3(35):

$$N(ads) + H \rightarrow NH(ads) \tag{33}$$

HCN and NH_3 probably explain the deficit observed in carbon and hydrogen balances. Moreover, NH_x formation can explain why there is no molecular hydrogen in zones B and C while hydrogen atoms are produced in these zones by several reactions.

5. DISCUSSION

Comparison of the reactions examined above with the experimental results allows us to point out some important features of the chemical mechanism of the methane–nitrogen cold plasma. A schematic mechanism would be the following:

$$\begin{tikzcd}
& CH_3 \arrow[r] & C_2H_6 \arrow[r] & C_2H_5 \arrow[r] & C_2H_4 \arrow[r] & \cdots \\
CH_4 + \text{plasma} \arrow[ur, "a"] \arrow[dr, "b"'] & & & & & \\
& CH_2, CH, C \arrow[r] \arrow[uurrr, "c"] & C_2H_2 \arrow[r] & \cdots & &
\end{tikzcd} \tag{34}$$

It is clear that C_2 hydrocarbons decompose when in contact with active species of the plasma as they are more reactive than methane. Path *b* needs more energetic conditions than path *a* and is not active when methane is added far from the cavity (zones B and C, $d > 1$ cm).

—C_2H_6 and C_2H_4 experimentally show a similar behavior, different from the behavior of C_2H_2. However, if we consider reactions (7)–(12), and (20)-(23) between *primary radicals* obtained from methane, ethane is produced via CH_3 [reaction (7)] while ethylene and acetylene come from C, CH, and CH_2 radicals [reactions (8)-(12) for ethylene and reactions (20)-(23) for acetylene]. To explain this apparent discrepancy, we suggest that ethylene is mainly obtained via reactions (8) and (19) involving *secondary* C_2H_5 *radicals* produced by dissociation of C_2H_6 and that path *c* is of less importance than path *a*;

—Since ethane is not detected in zone C, it must be supposed that the rate of reaction (7), ($k_7 \cdot [\text{methyl}]^2[\text{M}]$), is low in comparison with the rate of reaction (37), ($k_{37} \cdot [\text{methyl}] \cdot [\text{N}]$), into the far post-discharge. This would indicate that in this zone atomic nitrogen concentration [N] is still important.

—Dihydrogen is not observed in zones B and C, although several reactions previously quoted lead to H atoms. This experimental feature can be explained by reactions of atomic hydrogen on the wall with adsorbed N atoms [reaction (33)]; the reaction in the gas phase with methane [reaction (34) in Table I] shows a low rate constant in our experimental conditions.

—It is interesting to notice that propane and butane have been detected in very low concentrations in this work. The following reactions [competing with reactions (8) and (19)] can explain their formation:

$$C_2H_5 + CH_3 \overset{M}{\rightarrow} C_3H_8 \tag{35}$$

$$C_2H_5 + C_2H_5 \overset{M}{\rightarrow} C_4H_{10} \tag{36}$$

6. CONCLUSION

Conversion of methane to C_2 hydrocarbons has important industrial applications. For this purpose, we study the valorization of methane into a dinitrogen cold plasma. Our experiments indicate that the activation of methane by energetic electrons is necessary for acetylene formation, so the valorization of methane into the near post-discharge, where carbon deposition is weak, is an interesting way of conversion. In this study, we obtain 15% of acetylene in comparison with methane introduced (Fig. 7).

Results show that it is necessary to distinguish three main kinetic mechanisms corresponding to the three zones A, B, and C where methane undergoes a conversion into the end of the discharge or into the post-discharge of a dinitrogen plasma:

—zone A: Energetic electrons allow the formation of CH_2, CH, and C radicals [reaction (1)], so the formation of acetylene is observed [reactions (20)-(23)], while active dinitrogen produces methyl radicals [reactions (2a) and (3)], so ethane and ethylene are obtained [reactions (7), (10)-(16)], with some traces of propane [reaction (35)] and butane [reaction (36)]. Methanenitrile HCN is formed by reactions (24)–(29) and (37)–(38), and ammonia via reactions (30)–(33). Dihydrogen is mainly observed in this zone.

—zone B: The electron temperature is too low, so acetylene is not produced. Only active dinitrogen reacts with methane [reactions (2a) and (3)], so we observe the formation of ethane and ethylene [reactions (7) and (13)–(16)], of propane [reaction (35)], and of butane [reaction (36)]. HCN is obtained by reactions (24), (28), (37), and (38) and NH_3 via reaction (33).

—zone C: In this zone, neither hydrocarbons nor dihydrogen are detected, but a consumption of methane and of dinitrogen is observed [reactions (2a), (3), (24), (28), (33), (37), and (38)].

This microwave cold plasma technique developed for direct conversion of methane to C_2 compounds and particularly to acetylene has been patented.(45)

ACKNOWLEDGMENT

The financial support of Electricité de France for this work is gratefully acknowledged.

REFERENCES

1. F. Raulin, D. Mourey, and G. Toupance, *Origins Life* **12**, 267 (1982).
2. W. R. Thomson, T. J. Henry, J. M. Schwartz, B. N. Khare, and C. Sagan, *Icarus* **90**, 57 (1991).
3. M. E. Fraser, D. A. Fee, and R. S. Sheinson, *Plasma Chem. Plasma Process.* **5**, 163 (1985).
4. D. E. Tevault, *Plasma Chem. Plasma Process.* **5**, 369 (1985).
5. A. M. Diamy, J. C. Legrand, J. Al Andari, L. Hochard, and A. Ricard, *11th ESCAMPIG*, August 1992, St. Petersbourg (CEI), in *Europhysics Conference Abstracts* **16F**, 203 (1992).
6. H. Michel, *Interactions Plasmas Froids Materiaux*, Les Editions de Physique, Les Ulis (1987), p. 465.
7. J. Amouroux and D. Rapakoulias, *Rev. Phys. Appl.* **12**, 1013 (1977); D. Rapakoulias and J. Amouroux, *ibid.*, **14**, 961 (1979). P. Capezzuto, F. Cramarossa, G. Ferraro, P. Maione, and E. Molinari, *Gazz. Chim. Ital.* **103**, 1153 (1973). P. Capezzuto, F. Cramarossa, R. D'Agostino, and E. Molinari, *ibid.*, **103**, 1169 (1973).
8. A. Oumghar, J. C. Legrand, A. M. Diamy, N. Turillon, and R. I. Ben-Aïm, *10th Int. Symp. Plasma Chem., Bochum (Germany), Proc.* **3**, 2.3-7 (1991).
9. J. Weill, F. Chevron, C. Raimbault, R. Genier, G. Renesme, L. Capogna, and Y. Muller, *Rev. Inst. Fr. Pétrole* **47**, 255 (1992). J. H. Kiefer and S. S. Kumaran, *J. Phys. Chem.* **97**, 414 (1993).
10. J. Al Andari, A. M. Diamy, V. Hrachová, J. C. Legrand, and N. Turillon, *11th. Int. Symp. Plasma Chem., Loughborough (England), Proc.* **4**, 1344 (1993).
11. A. N. Wright and C. A. Winkler, *Active Nitrogen*, Academic Press, New York (1968).
12. P. Nectoux, R. Derai, and J. Danon, *Chem. Phys.* **37**, 229 (1979).
13. W. L. Morgan, *Plasma Chem. Plasma Process.* **12**, 477 (1992).

14. M. F. Golde, *Int. J. Chem. Kinet.* **20**, 751 (1988).
15. M. F. Golde, G. H. Ho, W. Tao, and J. M. Thomas, *J. Phys. Chem.* **93**, 1112 (1989).
16. A. N. Wright and C. A. Winkler, *Can. J. Chem.* **40**, 1291 (1962).
17. S. P. Walch and R. J. Duchovic, *J. Chem. Phys.* **90**, 3230 (1989).
18. M. Capitelli and E. Molinari, *Top. Curr. Chem.* **90**, 59 (1980).
19. M. Capitelli, C. Gorse, and A. Ricard, *Top. Curr. Phys.* **39**, 315 (1986).
20. A. Ricard, *Interactions Plasmas Froids Matériaux*, Les Editions de Physique, Les Ulis (1987), p. 241.
21. L. G. Piper, *J. Chem. Phys.* **87**, 1625 (1987).
22. W. J. Marinelli, W. J. Kessler, B. D. Green, and W. A. M. Blumberg, *J. Chem. Phys.* **90**, 2167 (1989).
23. D. L. Baulch, C. J. Cobos, R. A. Cox, C. Esser, P. Frank, T. Just, J. A. Kerr, M. J. Pilling, J. Troe, R. W. Walker, and J. Warnatz, *J. Phys. Chem. Ref. Data* **21**, 411 (1992).
24. P. Glarborg, J. A. Miller, and R. J. Kee, *Combust. Flame* **65**, 177 (1986).
25. F. L. Nesbitt, G. Marston, and L. J. Stief, *J. Phys. Chem.* **94**, 4946 (1990).
26. I. Messing, S. V. Filseth, C. M. Sadowski, and T. Carrington, *J. Chem. Phys.* **74**, 3874 (1981).
27. K. Schofield, *J. Phys. Chem. Ref. Data* **8**, 723 (1979).
28. B. Fell, I. V. Rivas, and D. L. McFadden, *J. Phys. Chem.* **85**, 224 (1981).
29. H. Umemoto, K. Sugiyama, S. Tsunashima, and S. Sato, *Bull. Chem. Soc. Jpn.* **58**, 3076 (1985).
30. M. Tichy, A. B. Rakshit, D. G. Lister, N. D. Twiddy, N. G. Adams, and D. Smith, *Int. J. Mass Spectrom. Ion Process.* **29**, 231 (1979).
31. K. Hiraoka, K. Aoyama, and K. Morise, *Can. J. Chem.* **63**, 2899 (1985).
32. J. Warnatz, Rate Coefficients in the C/H/O System, in *Combustion Chemistry*, W. C. Gardiner, Jr., ed., Springer-Verlag, New York (1984), Chap. 5, p. 197.
33. J. C. Mackie and K. R. Doolan, *Int. J. Chem. Kinet.* **16**, 525 (1984).
34. W. Braun, K. H. Welge, and J. R. McNesby, *J. Chem. Phys.* **45**, 2650 (1966).
35. K. S. Yin and M. Venugopalan, *Plasma Chem. Plasma Process* **3**, 343 (1983), M. Touvelle, J. L. Munoz Licea, and M. Venugopalan, *ibid.* **7**, 101 (1987).
36. H. Uyama and O. Matsumoto, *Plasma Chem. Plasma Process.* **9**, 13, 421 (1989). H. Uyama, T. Nakamura, S. Tanaka, and O. Matsumoto, *ibid.*, **13**, 117 (1993).
37. W. Tsang and R. F. Hampson, *J. Phys. Chem. Ref. Data* **15**, 1087 (1986).
38. W. Braun, J. R. McNesby, and A. M. Bass, *J. Chem. Phys.* **46**, 2071 (1967).
39. L. Herbert, I. W. M. Smith, and R. D. Spencer-Smith, *Int. J. Chem. Kinet.* **24**, 791 (1992).
40. A. J. Dean, R. K. Hanson, and C. T. Bowman, *J. Phys. Chem.* **95**, 3180 (1991).
41. W. A. Sanders and M. C. Lin, Kinetics and Mechanisms of Methylidyne Radical Reactions, in *Chemical Kinetics of Small Organic Radicals*, Z. B. Alfassi, ed., CRC Press, Boca Raton, Florida (1988), Vol. 3, p. 103.
42. C. P. Tsaï and D. L. McFadden, *J. Phys. Chem.* **94**, 3298 (1990).
43. J. Al Andari, A. M. Diamy, J. C. Legrand, and R. I. Ben-Aïm, *Plasma Chem. Plasma Process.* **13**, 103 (1993).
44. M. W. Chase, C. A. Davies, J. R. Downey, D. J. Frurip, R. A. McDonald, and A. N. Syverud, JANAF Thermochemical Tables, *J. Phys. Chem. Ref. Data* **14**, Suppl. No. 1, 1 (1985).
45. French Patent 92-01455 (1992).